

Detection of nitrification in amine modified multiwalled carbon nanotubes by TOF-SIMS ion imaging

Bhanu Pratap Singh & N Karar*

Division of Materials Physics and Engineering,
CSIR-National Physical Laboratory, Dr K S Krishnan Road, New Delhi 110 012, India
Email: nkarar@nplindia.org, bps@nplindia.org

Received 13 March 2015; accepted 29 July 2016

Nitrification of multiwalled carbon nano tubes (MWCNT) by mild oxidation with nitric acid has been reported. These acid functionalized tubes have been further refluxed with thionyl chloride leading to addition of amide groups followed by aromatic di-amine treatment. Formation of such nitrated material have been initially confirmed by SEM, HR-TEM, Raman and Infrared (FT-IR) spectra. Such nitration are further cross-checked and confirmed using Time of Flight Secondary ion mass spectrometry (TOF-SIMS) based ion imaging, which revealed presence of different nitrogen related groups. TOF-SIMS also detected traces of some of the residues and impurities created during the process steps.

Keywords: MWCNT, Amidation, TOF-SIMS, Ion Imaging

Due to its exceptional mechanical properties, carbon nanotubes (CNTs) have attracted a lot of attention for its use as reinforcement with the different polymeric systems for enhancing the physical properties¹. Unfortunately, as-synthesized CNTs are insoluble in all the solvents. Therefore their interaction, bonding or adhesion with any polymer is very poor. Consequently, the mechanical properties of CNTs based polymer composites could not been fully exploited. Thus tailoring the surface properties of multiwalled carbon nano tubes (MWCNT) is an emerging challenge for successful commercial viability of MWCNT based products. Amine modification of carbon nanotubes (CNT) leads to some defects and dangling bonds but the unsaturated bonds are engaged with the nitrides. So chemical functionalization is the easiest way to modify the surface of CNTs with some functional groups. These are compatible with many of the commonly used polymer matrices. An epoxy thermosetting resin is a combination of prepolymer (generally in the form of di-glycidyl ether of bisphenol A) and cross linking agent-hardener (preferably in the form of an amine). Therefore, as a corollary, amino functionalization of CNTs using such a thermosetting resin is also expected to enhance the interaction/bonding between the CNTs and such an epoxy through the covalent linkage which can enhance the mechanical properties. Amine

modification should also improve dispersion and interfacial adhesion of CNTs to the epoxy resin. Several studies have reported amine modified MWCNTs (Am-MWCNT) as reinforcement with the epoxy resin and significant improvement in the mechanical properties have been observed with respect to non functionalized MWCNTs (o-MWCNT)². Such an amine modification is a three step process viz. i). Oxidation, ii). Chlorination, iii). Amidation (Am). An understanding of the characteristics of such amine modified MWCNTs is important for its utility prospects.

Several authors have reported functionalization of MWCNTs using different type of amines. Yang *et al.* used triethylene tetramine for amine functionalization of MWCNT³. Delmotte also used similar amine for surface modification of MWCNTs but these amine modified MWCNTs were reinforced with epoxy resin which significantly enhanced mechanical properties². Similarly, Singh *et al.* used octadocyl amine for the attachment of amine groups and these were reinforced with polyimide⁴. Gojny *et al.* also used amino functional CNTs where SWCNTs, DWCNTs and MWCNTs were ball milled in the presence of ammonia and used as reinforcement with epoxy resin⁵. In all these studies, including the one done by Singh *et al.*⁶, amine modified CNTs were most characterized by FTIR, Raman spectroscopy, SEM, TEM, EDX, CHNS, XPS, and TGA.

Time of Flight Secondary Ion Mass Spectrometry (TOF-SIMS) is an important characterization technique used for analysis of constituents and impurities. Its full usage potential has not been explored so far for the characterization of Am-MWCNTs. It has a very good impurities' detection limit of up to ppm and at times ppb, and has been used semi-quantitatively in a routine way to check properties like composition, uniformity, doping levels in biological, metallurgy and semiconductor industry. Availability of standard samples for comparison can further improve the quantification process. Here we also report on a TOF-SIMS ion image based study of Am-MWCNTs to cross-check nitrification. TOF-SIMS is used to show that nitrification of MWCNT can also be detected by this technique after comparison with nonamide samples. Though it is not a replacement for XPS, at times, the ion imaging mode of TOF-SIMS⁷ can be used for complimentary information like extent of uniformity of amidation and homogeneity. This will be obvious from subsequent discussions. Since amine modification is nitration of MWCNT, these two words have been used in a synonymous analogous manner.

Experimental Section

Synthesis

MWCNTs were synthesized using toluene as a carbon source and ferrocene as catalyst in a chemical vapour deposition (CVD) set-up developed in the laboratory. The MWCNTs produced were of ~26 nm average diameter. These have been designated as o-MWCNTs. The details of this experimental set-up are given elsewhere⁸.

Chemical modification of MWCNTs

Chemical modifications of MWCNTs were carried out by oxidation using nitric acid treatment (oxidation) by refluxing 1 g of as-produced MWCNTs with 200 mL concentrated nitric acid (60% (v/v)) for 24h at 70°C and then cooled down to room temperature. The thoroughly washed MWCNTs were dried overnight at 110°C. Acid modified MWCNTs 1 g was dispersed in 30 mL of anhydrous benzene (C₆H₆) and 30 mL of thionyl chloride (SOCl₂) and was refluxed for 10 h leading to chlorinated MWCNTs formation. COCl-MWCNTs (0.5 g) was then suspended in tetra-hydro furan (THF) and refluxed with excess Aradur 5200 (aromatic diamine) for 90 h to produce amine modified MWCNTs⁹. This amine modified MWCNTs was designated Am-MWCNTs.

Characterization

The surface morphology of as produced MWCNT, Am-MWCNTs was analyzed using scanning electron microscopy (SEM, Zeiss EVO MA-10). HRTEM studies of as, o-MWCNTs and Am-MWCNTs were carried out using Tecnai G20-stwin, 300 kV instrument. TOF-SIMS measurements were done for their ion content and distribution analysis at room temperature using an Ion-TOF-V-100 instrument with a Bi⁺ ion source operated at 25keV by collecting mass spectra data for 5.5 min in each case. The rastered area and signal detection was from 100 μm × 100 μm region. High current bunched mode (HCBM) was used. Such issues have been discussed in the paper by Todd *et al.*¹⁰. The pixel size was chosen as 2048 × 2048 over this 100 μm × 100 μm region, with one shot per pixel in random mode to reduce charging effects. Bi⁺ was chosen as it has a much higher current than the Bi³⁺. The Bi⁺ ion current was about 1pA. Such pixel size (50 nm) was chosen to try and increase information content spatially. Samples for analysis were made into very thin sheets and were in contact with metal plates and sample holder to reduce charging effects. Appropriate charge neutralization mechanisms were used and further optimized with the operating software to avoid charging of the samples during data collection. Mass calibration, identification of ions species and associated activities were done using SurfaceLab6 software from M/S IonTOF GmbH.

Results and Discussion

Surface Morphology

Figures 1a and 1b show the SEM micrographs of o-MWCNTs and Am-MWCNTs respectively. As can be seen in Fig. 1a, the o-MWCNTs are in the form of long MWCNTs. Treatment of MWCNTs with strong acids followed by amine treatment usually shortens the length of the MWCNT¹¹ due to resultant breaking of some of the chemical bonds. In the present study, we have also observed such shortening of the tube length. A closer look at the micrographs reveals that the amino functionalized MWCNTs (Fig. 1b) are relatively shorter compared to o-MWCNTs (Fig. 1a). The surface of Am-MWCNTs is also roughened compared to o-MWCNTs which are due to the attachment of functional groups. The surface roughness of the MWCNTs during amine functionalization were further confirmed by HRTEM studies (Figs 2a and 2b for o-MWCNTs and

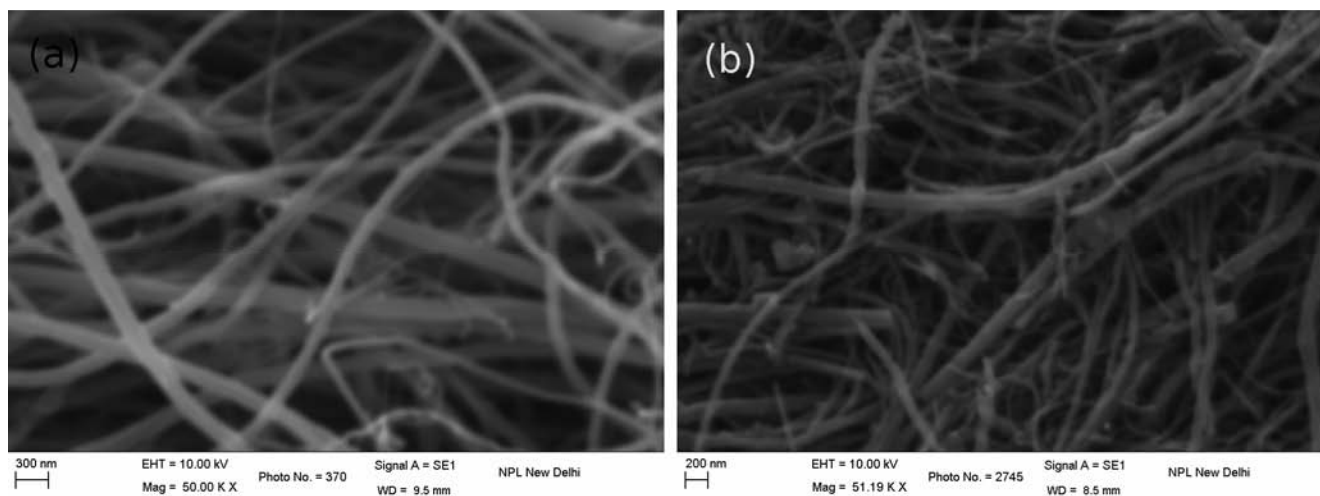


Fig. 1 — (a) SEM image of o-MWCNT; (b) SEM image of Am-MWCNT

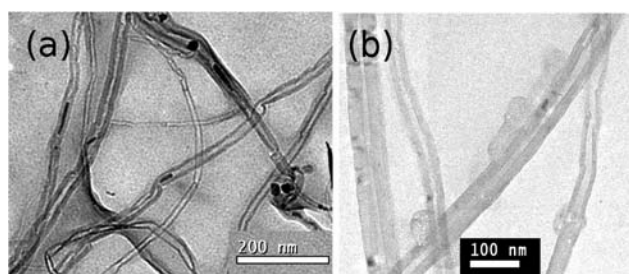


Fig. 2 — (a) TEM image of o-MWCNT; (b) TEM image of Am-MWCNT

Am-MWCNTs, respectively). HRTEM images of the Am-MWCNTs suggest that the surface roughness of Am-MWCNT (Fig. 2b) is much higher than the o-MWCNT (Fig. 2a). The surface roughness can therefore be attributed to the presence of functional groups. Therefore, shortening of the length and pronounced surface roughness of CNTs are due to the attachment of functional groups.

FTIR is an important tool for the identification of functional groups in organic compounds. It has been used for characterization of amine modified MWCNT by several authors^{2,6}. FTIR spectrum from aromatic diamine modified MWCNTs suggested presence of amine based groups i.e the peaks at 1263 cm^{-1} and 1448 cm^{-1} were ascribed to C–N stretching of amide groups, while the peak at 3396 cm^{-1} can be assigned to the N–H stretching vibrations. The peaks at 1622 and 1371 cm^{-1} correspond to the N–H bending and C–N stretching of amine respectively^{6,11,12}.

Raman spectroscopy:

Figure 3 shows the Raman spectra of o-MWCNTs (Fig. 3a), Acid-MWCNTs (Fig. 3b) and Am-

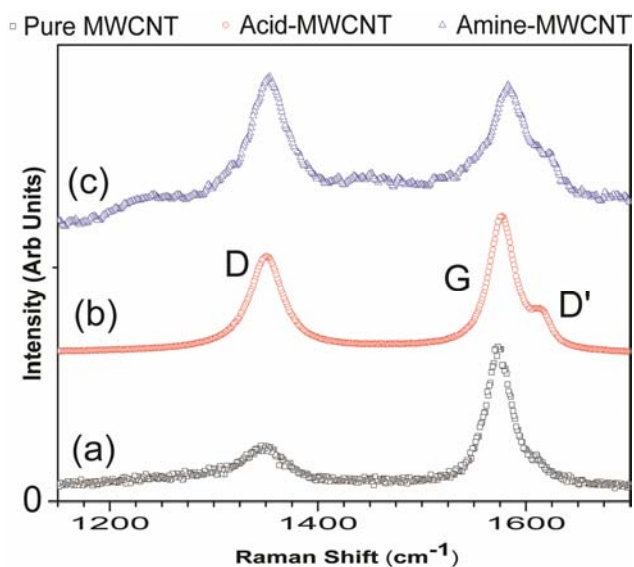


Fig. 3 — Raman spectra of (a) o-MWCNTs, (b) Acid-MWCNTs and (c) Am-MWCNTs

MWCNTs (Fig. 3c). Associated comparison in the Raman shift and I_D/I_G ratio of these different types of MWCNTs are presented in Table 1. There are three distinct peaks in all the spectra. The first is the D band, which is induced by the structural disorder of the tubes and are located at 1343 , 1350 and 1350 cm^{-1} for o-MWCNTs, Acid-MWCNTs and Am-MWCNTs respectively, (Table 1). There is a small shoulder at around 1230 cm^{-1} only in the amine modified sample. It is possibly related to the aminification related bonds¹². The second peak, the G band is associated with the tangential stretching mode of the graphitic C=C bond and is located at 1573 , 1577 and 1583 cm^{-1} for o-MWCNTs, Acid-MWCNTs, and Am-MWCNTs

respectively. The third peak appears in the spectra as a shoulder of the G-band at the higher frequency side. This feature is observed at 1617 cm^{-1} in o-MWCNT, 1615 cm^{-1} in Acid-MWCNT and 1620 cm^{-1} in Am-MWCNTs samples (Table 1) and is designated as the D' band¹². Similar to the D band, the D' band originates from a double resonance Raman process induced by structural disorder^{12,13}. Thus, the intensities of the D (I_D) and D' ($I_{D'}$) bands are associated with the presence of defects on the nanotubes, while the G band intensity (I_G) is independent of structural disorder. Herein, a significant change in the I_D/I_G ratio is observed in the Raman spectra and tabulated in Table 1. The I_D/I_G is 0.390 for o-MWCNTs, 0.704 for Acid-MWCNTs and

1.26 for Am-MWCNTs, respectively. The systematic increase in the I_D/I_G ratio with nitrification further confirms the attachment of functional groups generated during acid and amine treatment.

Detecting nitrogen in low quantities using secondary ion mass spectrometry is a little complicated, especially as in the present case, since the expected nitrification is about 8 to 10% or so, as some of these ion species are often detected only in certain combination ion modes. Here we have used positive and negative time of flight mass spectrometry (TOF-SIMS) and related ion imaging to detect the combinatorial nitrogen mass peaks, with other mass fragments to decisively show presence of nitrogen and nitrification of CNT with the relevant mass peaks from residues corresponding to its different preparation stages as discussed earlier (Figs 4, 5, 6). The mass calibration for positive spectra of CNT sheets were done by considering the ion peaks of H^+ , HH^+ , C^+ , CH_3^+ , $C_2H_3^+$, $C_3H_3^+$, $C_3H_7^+$, $C_4H_7^+$, $C_5H_7^+$, $C_6H_5^+$, $C_9H_7^+$, while the mass calibration of negative spectra of the CNT sheets were done by considering the ion peaks of H^- , HH^- , C^- , CH^- , CH_2^- , O^- , C_2H^- , CH_3^- , C_2^- , $C_2H_3^-$, C_3^- , C_3H^- , C_4^- ,

Table 1 — Table showing Raman spectral positions of MWCNT after nitrification

Band	o-MWCNTs	COOH-MWCNTs	Am-MWCNTs
D Band, (cm^{-1})	1343	1350	1350
G Band, (cm^{-1})	1573	1577	1583
D' Band, (cm^{-1})	1617	1615	1620
I_D/I_G	0.390	0.704	1.26

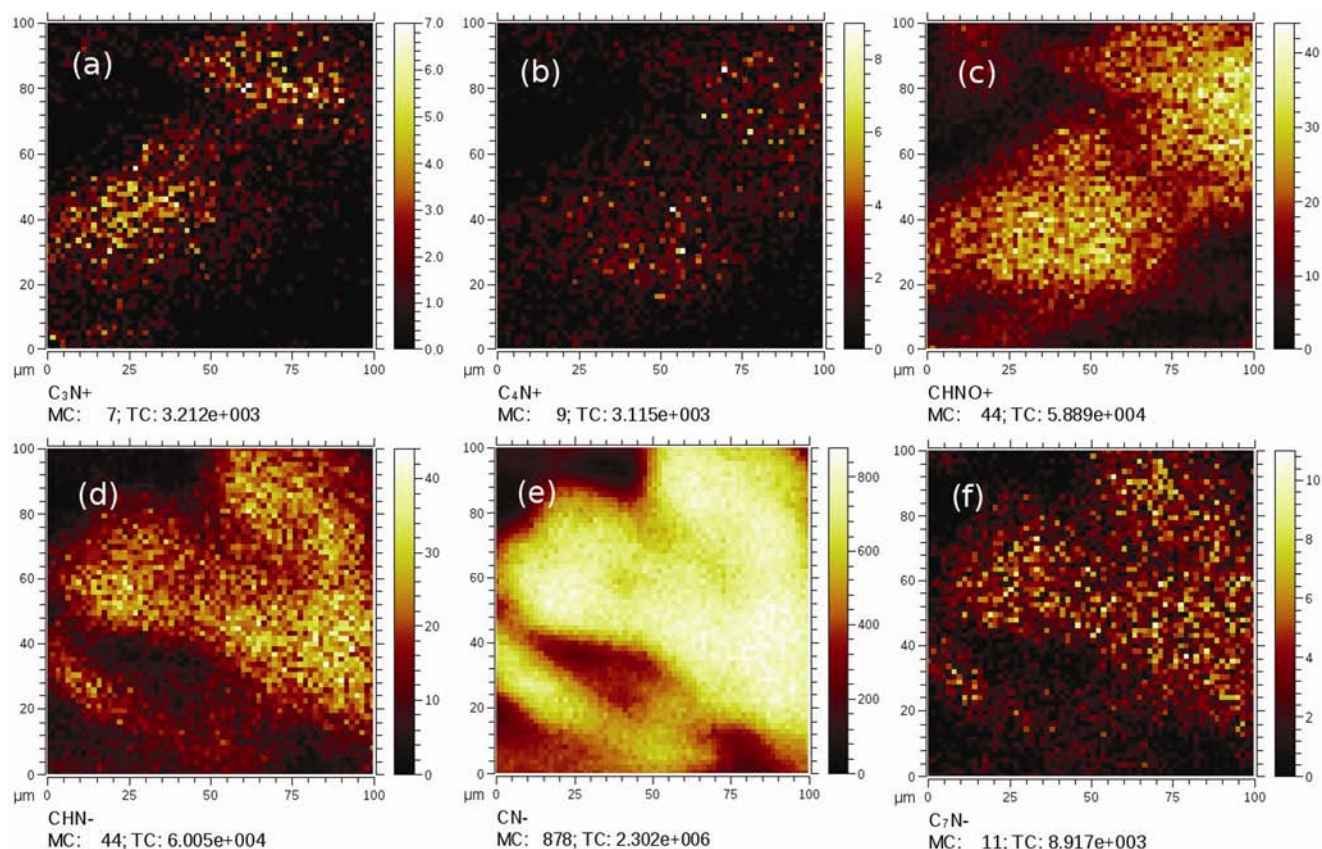


Fig. 4 — Ion images for a few representative ions in both positive and negative spectra for nitrated MWCNT

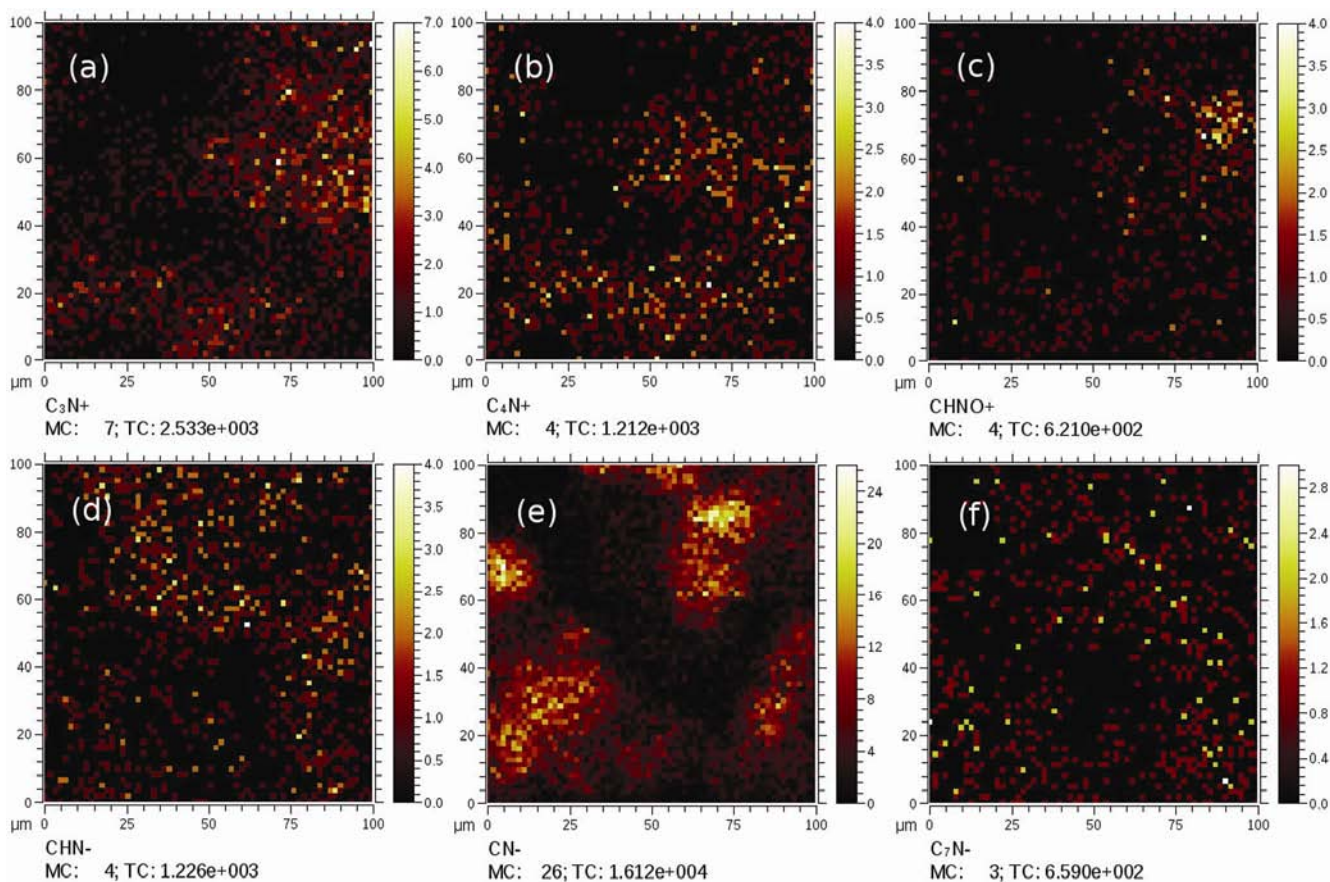


Fig. 5 — Ion images for a few representative ions in both positive and negative spectra for pure MWCNT, for comparison with ion images and related ion counts from nitrated MWCNT of Fig.4. This is due to commercial grade raw materials used during preparation and resultant presence of high impurities.

C_4H^- , C_5H^- , C_6^- , C_6H^- ¹⁴. The elemental composition analysis of the relatively stronger peaks or possible peaks of interest based on which an ion image pattern is discussed subsequently below were done based on a good mass calibration as above and subsequent software assisted checking for ion species identification in each case. The ions observed and discussed below are based on interaction between the Bi⁺ beam and the sample surface and the resultant preferential break up of the sample surface, their ionization and subsequent detection. So certain ion fragments are preferably seen with respect to others and that depends on the chemical or polymeric composition of the sample surface. Hence the nitrogen based fragments are preferentially observed and discussed as below.

Repeatability of mass spectrometry and ion image data was checked. Uniformity of ion images having non-negligible counts from C_3N^+ , C_4N^+ , $CHNO^+$ in the positive spectral images and CHN^- , CN^- , C_7N^- in negative spectral images suggest nitrification of

the CNT (Fig. 4). Corresponding change in CNT properties may now be accounted for beyond doubt due to nitrification. Some of the combination ion clusters are detectable and give higher counts only as positive ions (eg. C_3N^+ , C_4N^+ , $CHNO^+$ etc) while in some other cases such other ion clusters are detected and have higher counts only as negative ions (eg. CHN^- , CN^- , C_7N^- etc). Hence both type of ions had to be considered here (Figs 4, 5). The surface features for all the positive spectral ion images are similar and so is the case with the negative ion images (Figs 4, 5). The positive and negative ion images have been taken from different spots - so they look different. However even in the same spot, since the relative counts of different ions are different, the relative clarity of different ions' related images may at times be different, though broadly their shapes are similar. Since the relative yield of the different ions is different, their relative intensities are also different. That is to be expected since the sample area they represent have these surface features. The ion images

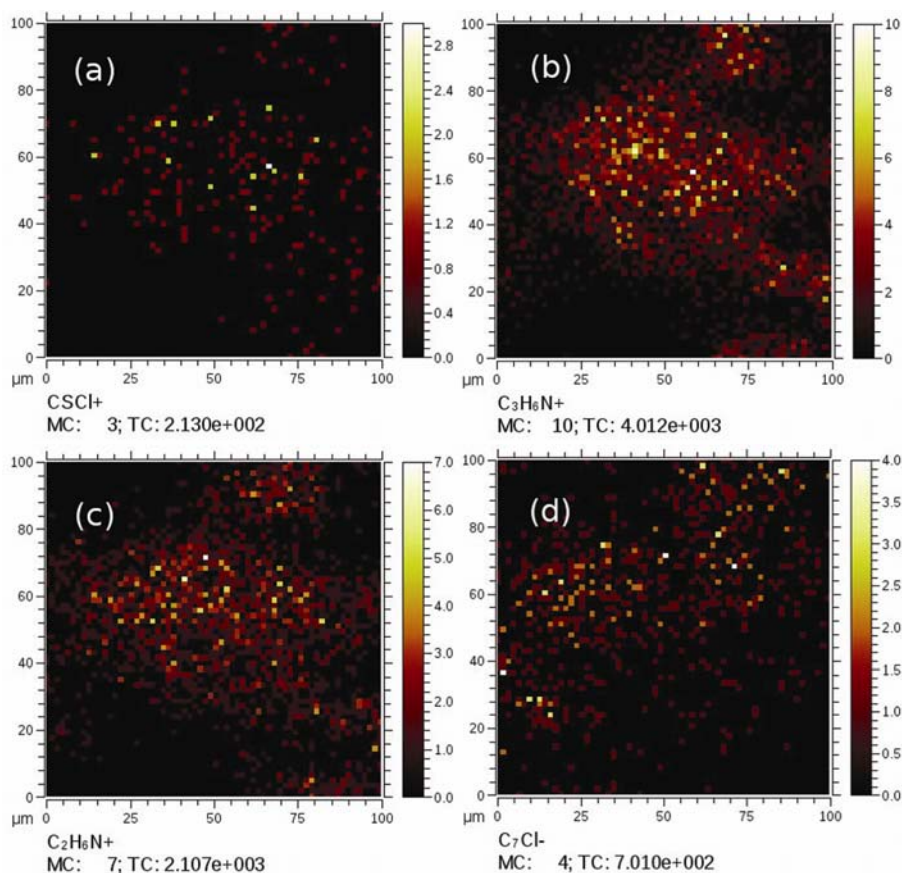


Fig. 6 — Representative ion images from reactant residues in the sample from the different process steps, the ion species are visible in the respective image caption.

for the corresponding un-nitrated CNT are also shown in Fig. 5 for a relative comparison. Nitrification of CNT increased the ion counts by almost two orders of magnitude in some cases. All ion images could not be accommodated in Fig. 4 or Fig. 5. The relatively poor ion counts observed in ion images of un-nitrated CNT (Fig. 5) are also due to the usage of commercial grade reactants for CNT preparation and resultant presence of impurities. The extent of homogeneity is also visible from such ion images. Incidentally, ion images with different counts corresponding to intermediate reactant ions like $C_xNO_3^+$, C_xSOCl^+ were not visible. However, traces of a little C_xSCl^+ , C_7Cl^- , (where x is a positive integer) were also visible (Fig. 6) while the ion counts from the final reactants $C_xH_6N^+$ were much stronger. These are possibly residues from the three step preparation process (Fig. 6) and could be detected due to ppm impurity detection ability of TOF-SIMS; eg. the chloride related ions come from the thionyl chloride and $C_xH_6N^+$ from benzene used in the process as discussed in the experimental part earlier. So we are now able to show that in an

independent way without XPS data, nitration of MWCNT could be observed experimentally using the positive and negative ion imaging mode of TOF-SIMS.

Conclusion

In summary, MWCNT has been tailored by attaching amino functional groups through a three step process which was confirmed by TEM, Raman and FTIR. These results also suggest that molecular length of MWCNT decrease and surface roughness increase with such nitration due to breakage of some of the bonds during the reaction process. TOF-SIMS ion imaging has also been used to confirm the success of nitration process further. It showed presence of different positive and negative nitrated carbon ion fragments. Traces of impurities from different stages of nitration process are also detected from the TOF-SIMS ion images. The homogeneity of the nitrated MWCNT is also conformed from these ion images. Since nitration of MWCNT is now proven using TOF-SIMS, such TOF-SIMS based

analytical techniques can perhaps be further used in analysis of many other similar tailored carbon bearing materials in future.

Acknowledgements

The authors thank K.N. Sood of CSIR-NPL for SEM. Funding from the CSIR network research project PSC-0109 is acknowledged.

References

- 1 Mittal V, *Polymer Nanotube Nanocomposites: Synthesis, Properties, and Applications* (John Wiley & Sons) 11 (2010).
- 2 Delmotte J & Rubio A, *Carbon*, 40 (2002) 1729.
- 3 Yang K, Gu M, Guo Y, Pan X & Mu G, *Carbon*, 47 (2009) 1723.
- 4 Singh B, Singh D, Mathur R & Dhama T, *Nanoscale Research Lett*, 3 (2008) 444.
- 5 Gojny F H, Wichmann M H G, Fiedler B & Schulte K, *Composites Science and Technology*, 65 (2005) 2300.
- 6 Singh B P, Choudhary V, Teotia S, Gupta T, Singh V, Dhakate S & Mathur R, *Adv Materials Lett*, 6 (2015) 104.
- 7 Briggs D, & Vickerman J, *ToF-SIMS: Materials Analysis by Mass Spectrometry* (IM Publications, London) 2nd Edn (2013).
- 8 Singh B P, Saini K, Choudhary K, Teotia S, Pande S, Saini P & Mathur R B, *J Nanoparticle Res*, 16 (2014) 2161.
- 9 Stobinski L, Lesiak B, Kover L, Toth J, Biniak S, Trykowski G & Judek J, *J Alloys Compounds*, 501 (2010) 77.
- 10 Todd P J, Schaaff T G, Chaurand P & Caprioli R M, *J Mass Spectrometry*, 36 (2001) 355.
- 11 Marshall M W, Popa-Nita S & Shapter J G, *Carbon*, 44 (2006) 1137.
- 12 Kim J, Furtado C, Liu X, Chen G & Eklund P, *J Am Chem Soc*, 127 (2005) 15437.
- 13 Silva W M, Ribeiro H, Seara L M, Calado H D, Ferlauto A S, Paniago R M, Leite C F & Silva G, *J Brazilian Chem Soc*, 23 (2012) 1078.
- 14 Karar N & Gupta T, *Vacuum*, 111 (2015) 119.